

ELECTRIFICATION AND LIGHTNING IN A SIMULATED SUPERCELL THUNDERSTORM

C. L. Ziegler¹, E.R. Mansell³, D. R. MacGorman¹, and J. M. Straka²

¹National Severe Storms Laboratory (NSSL), Norman, Oklahoma, U.S.A.

²School of Meteorology, University of Oklahoma (OU), Norman, Oklahoma, U.S.A.

³Cooperative Institute for Mesoscale Meteorological Studies/OU, Norman, Oklahoma, USA.

ABSTRACT: This study reports results of electrification and lightning evolution in a supercell storm simulated with the OU/NSSL three-dimensional storm electrification model. A series of 3-hour storm simulations have been performed, changing the non-inductive charging scheme from run to run to examine their impact on simulated electrification and lightning. Charge regions were elevated in the main updraft relative to surroundings, in agreement with earlier studies. Subsequent simulated electrification was very intense, with total lightning rates exceeding 200 flashes/min in the supercell storm after 3 hours. Frequent ground flashes were simulated, with polarity dependent on the non-inductive charging scheme being employed, and peak CG rates exceeded 10 flashes/min. Trends are suggested between updraft intensity, graupel volume, and total lightning rates.

Introduction

In a previous study using a kinematic numerical model, we evaluated the role of non-inductive graupel-ice charging and explored the relationships between space charge, electric fields, and lightning morphology at the mature stage of the tornadic Binger, OK supercell storm (Ziegler and MacGorman 1994). However, large or rapidly moving storms and storm systems are not usually observed with Doppler radars to the extent required by the time-varying kinematic model. To study storm evolution processes, we have conducted simulations of a supercell storm in the same environment as the Binger storm using the OU-NSSL 3-dimensional, time-dependent storm electrification model.

Our three-dimensional cloud model employs non-hydrostatic and fully compressible airflow dynamics, including prognostic equations for three momentum components, pressure, potential temperature, and turbulent kinetic energy. There are additional conservation equations for mixing ratios of water vapor and hydrometeors and age of cloud parcels. The model also explicitly solves conservation equations for ion and hydrometeor charge densities. A wide variety of warm- and cold-cloud microphysical processes are represented via bulk parameterizations.

A range of ion and hydrometeor charging processes and a branched lightning parameterization are incorporated in the model. Mansell et. al. (2003, this volume) gives details of the electrification mechanisms and their relation to the microphysics. In the two simulations presented here, we alternately employ the "Gardiner/Ziegler" (GARD) or the "Saunders/Peck-1998" rime accretion rate (SP98) noninductive charging schemes. Other charging mechanisms (e.g. strong inductive graupel-ice charging) are treated identically in both runs. Additional simulations with the optional Takahashi and riming rate (RR) noninductive charging schemes will be reported at the conference.

The Binger storm initiated east of the dryline in SW Oklahoma at 1930 UTC on 22 May 1981 (MacGorman et al. 1989). Over the next three hours it moved northeastward and intensified, producing the first of five tornadoes around 2230. The Binger storm produced 79 negative cloud-to-ground (-CG) flashes (no +CGs) between 2100 and 2230, and produced four more tornadoes and frequent lightning over the next three hours. The present study concentrates on the storm's electrification during the first 3 hours.

The simulated supercell storm is initialized in a horizontally homogeneous base state environment derived from an observed sounding in the Binger storm's environment at 2015 UTC. The input sounding has over 4000 J kg⁻¹ of convective available potential energy (CAPE), strong directional turning of the hodograph in the lowest 3 km, and a storm-relative helicity of 270 m² s⁻². The simulations are performed in a 110-km x 110-km x 22.5-km domain with constant horizontal spacing of 1 km and vertical spacing that stretches from 100 m at the ground to 500 m aloft. Vertical motion is initiated by introducing a randomized

warm thermal bubble with an amplitude of 2.5 °C, horizontal and vertical radii of 8 and 1.5 km respectively, and an elevation of 1.5 km AGL. The model is integrated for a period of 3 hours in a storm-relative reference frame moving northeast at 10 ms⁻¹.

Results and Discussion

The storm develops rapidly during the first 20-30 min, and subsequently intensifies in two main stages (Fig. 1a). During the first 100 min, updrafts and electric fields achieve average peak values of about 45 ms⁻¹ and 80 kVm⁻¹, respectively, as storm-integrated graupel mass slowly increases. Rain mass in the first 100 min is negligible during this "low-precipitation" (LP) stage (Fig. 1a). The storm intensifies after 100 min, achieving an average peak updraft of about 60 ms⁻¹. Both graupel and rain masses increase during the latter "high-precipitation" (HP) intensification stage, as the peak electric field increases to over 100 kVm⁻¹.

After 20 min, intracloud (IC) discharges commence at about 1-2 flashes min⁻¹ and increase to 25 flashes min⁻¹ by 100 min (GARD curve "IC1", Fig. 1b). During the subsequent HP stage after 100 min, the IC flash rates increase steadily to about 200 flashes min⁻¹. The IC flash rate exhibits a strong correlation with graupel volume, indicative of the dominant influence of non-inductive graupel-ice charging. The SP98 non-inductive charging scheme results in very similar IC flash rates to the GARD scheme (SP98 curve "IC2", Fig. 1b).

During the subsequent HP phase after 100 min, the storm develops a broader, deeper convective region, a low-level cumulus "flanking line", an "overshooting" storm top, and a "back-sheared" anvil cloud (Fig. 2). The GARD model run produces a negative-positive-negative lightning leader polarity arrangement with height (Fig. 2), corresponding to a conventional tripolar net space charge profile. Three flash types (aggregated in Fig. 2) associate with the GARD model run: high-level ICs with negative-below-positive leaders (ie. "+/-" polarity); low- and mid-level -/+ ICs; and low-level negative cloud-to-ground (-CG) discharges (e.g. one -CG each in Figs 1a-b). Figs. 2 and 1b consistently indicate that IC flashes tend to be restricted toward the convective storm core.

The GARD and SP98 model runs exhibit opposite lightning leader segment polarity, and by implication also opposite net charge profiles (Fig. 3). Consistent with Fig. 2, the GARD model run produces a tripolar negative-positive-negative (i.e. "-/+/-") leader profile. Conversely, the SP98 model run produces a tripolar "+/-/+" profile. The GARD simulation produced 11,766 ICs and 72 -CGs (no +CGs), in good agreement with observations, while the SP98 simulation produced 9,339 ICs and 126 +CGs (no -CGs). Inspection of other model output fields (not shown) strongly suggests that the transient development of lower positive (negative) charge centers immediately precedes and initiates the simulated negative (positive) ground flashes.

The intense, sustained simulated supercell updraft elevates main net charge regions (Fig. 4), as previously hypothesized based on earlier kinematic model results for the Binger, Oklahoma tornadic storm (Ziegler and MacGorman 1994). Simulated electric field meter (EFM) soundings "launching" at 2h 23 m are obtained for the GARD and SP98 model runs through the updraft core (Fig. 4). In the GARD model run, the simulated EFM updraft sounding has a main negative charge in the 9-14 km layer (Fig. 4a) but has positive leaders concentrated in the 4-11 km layer through the storm generally (Fig. 3a). Analogously for the SP98 model run (but with opposite polarity), the simulated EFM updraft sounding has a main positive charge in the 7-9 km layer (Fig. 4b) but has negative leaders concentrated more broadly in the 4-12 km layer through the storm generally (Fig. 3b).

The different non-inductive charging schemes employed in the GARD and SP98 model runs force marked differences in the net charges and lightning polarities of the simulated storms. The GARD non-inductive charging produces main positive and negative charge centers on graupel, with the maximum positive graupel charge around the reversal temperature (-15 °C) and with an upper positive charge on ice crystals. The SP98 non-inductive charging produces a colder reversal temperature in the moderate supercooled cloud water contents and riming rates in the main updraft. As a result of these moderate riming rates in the simulated updraft core, the SP98 scheme tends to produce elevated main positive and negative graupel charge cores in the simulated updraft in comparison to the GARD model run. The GARD and SP98 simulated EFM updraft soundings also have weak

positive (negative) net charges and electric fields from the surface through 6 km, suggesting weak recycling and horizontal entrainment of charged precipitation to "seed" the 0-6 km updraft core.

Future Work

Important foci of our research are to determine electrification processes and to isolate the factors controlling the triggering and polarity of simulated CG flashes in supercell and multicell storms and mesoscale convective systems (MCSs). All simulation results are being combined to determine empirical relationships between various measures of convective intensity and total lightning, with results applicable to our ongoing work to assimilate lightning observations into mesoscale weather prediction models.

Acknowledgements: This research was supported by NSSL and the Cooperative Institute for Mesoscale Meteorological Studies of the University of Oklahoma and by NSF grant ATM-0119398.

References

- MacGorman, D. R., D. W. Burgess, V. Mazur, W. D. Rust, W. L. Taylor, and B. C. Johnson, 1989: Lightning rates relative to tornadic storm evolution on 22 May 1981. *J. Atmos. Sci.*, **46**, 221-250.
- Mansell, E.R., D. MacGorman, J. M. Straka, and C.L. Ziegler, 2003: Recent results from thunderstorm electrification modeling. *Proc. 12th Intl. Conf. on Atmos. Elec. (ICAE '03)*, Versailles, France, this volume.
- Ziegler, C. L., and D. R. MacGorman, 1994: Observed lightning morphology relative to modeled space charge and electric field distributions in a tornadic storm. *J. Atmos. Sci.*, **51**, 833-851.

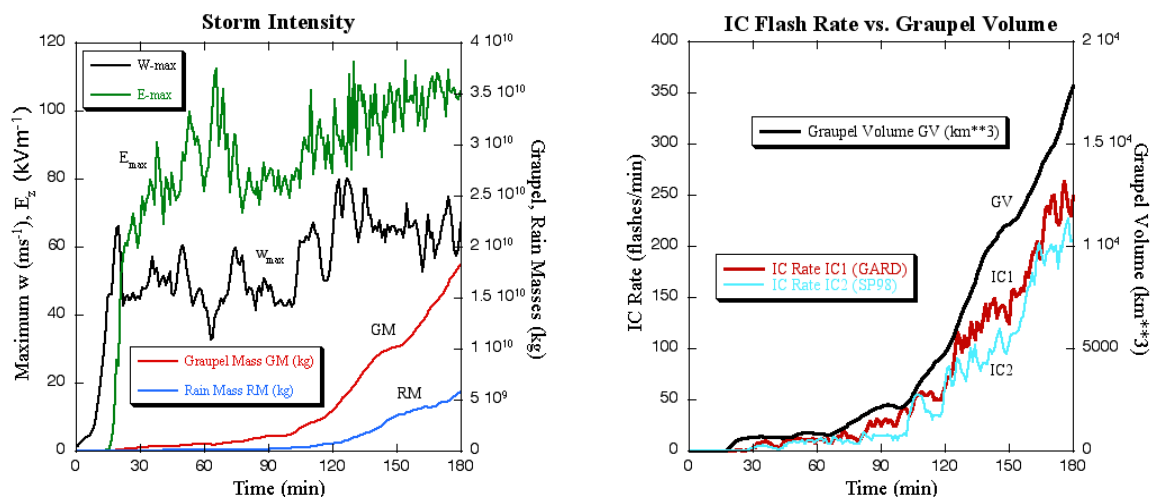


Figure 1. Time series of (a - left) vertical velocity and peak vertical electric field, and (b - right) simulated graupel volume (km³) versus intra-cloud (IC) flash rates (min⁻¹) for model runs employing Gardiner-Ziegler (GARD) and Saunders and Peck 1998 (SP98) non-inductive graupel-ice charging.

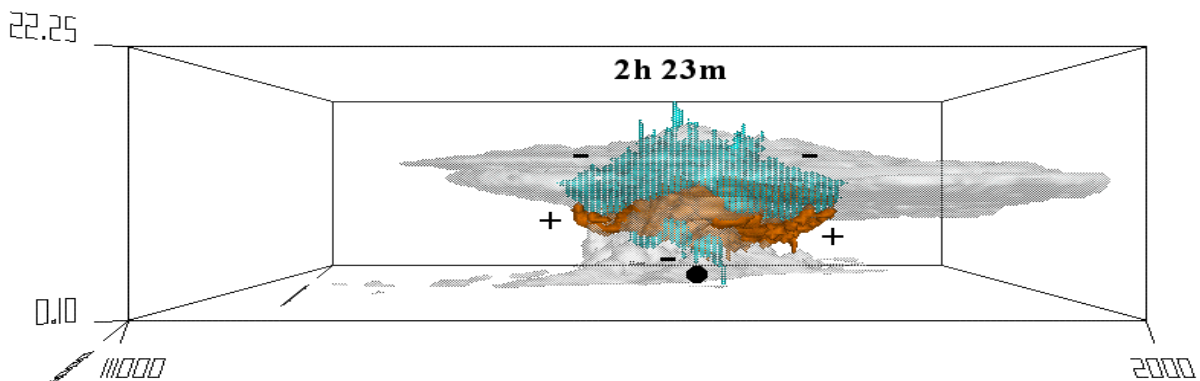


Figure 2. View of the high-precipitation (HP) supercell at 2h 23m into the simulation, looking north. The cloud (water and ice) edge is denoted by the light gray surface. Plus and minus signs indicate polarity of adjacent volumes containing positive (red/dark gray) and negative (blue/medium gray) leaders. The heavy dot indicates the launch location of the simulated soundings depicted in Figure 4.

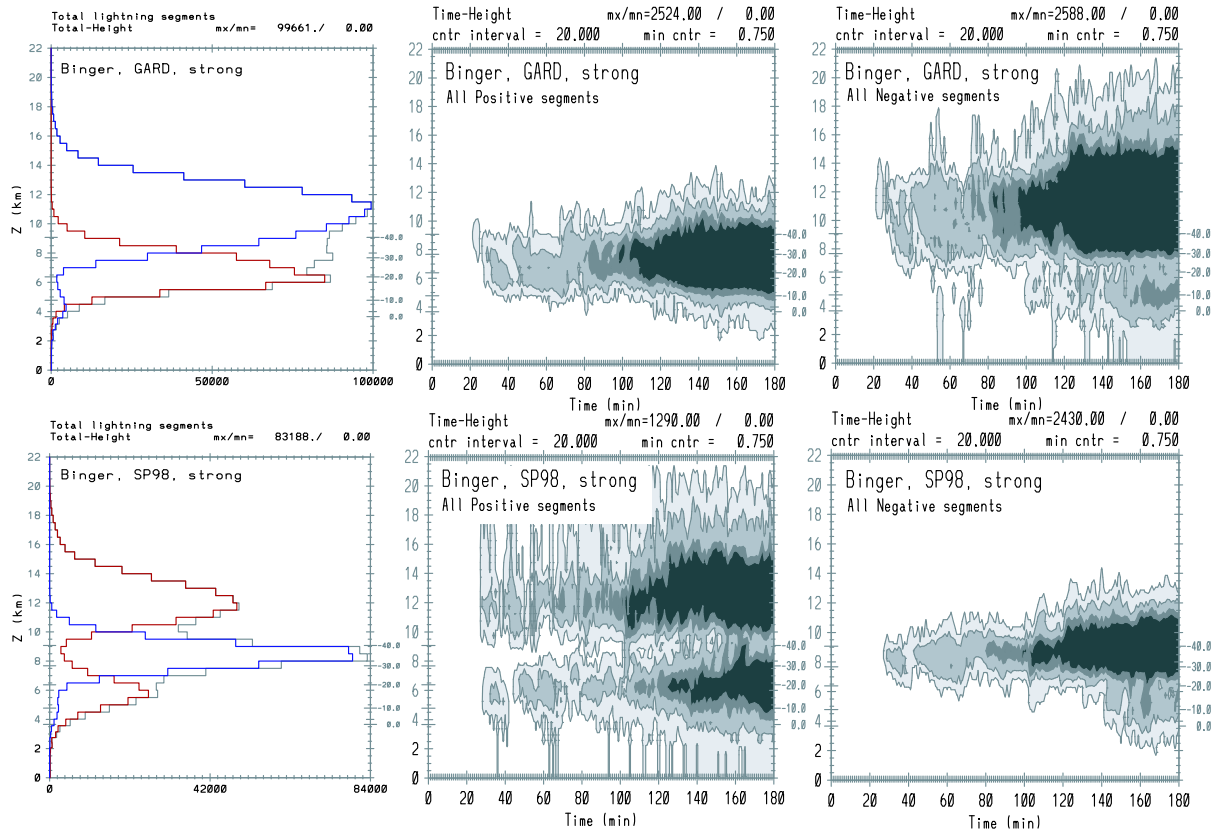


Figure 3. Time-height sections of lightning leader segments per grid cell for runs (a - top) GARD and (b - bottom) SP98 over the duration of the 3 hour simulation. Left column: total lightning segments; center column: all positive segments; right column: all negative segments.

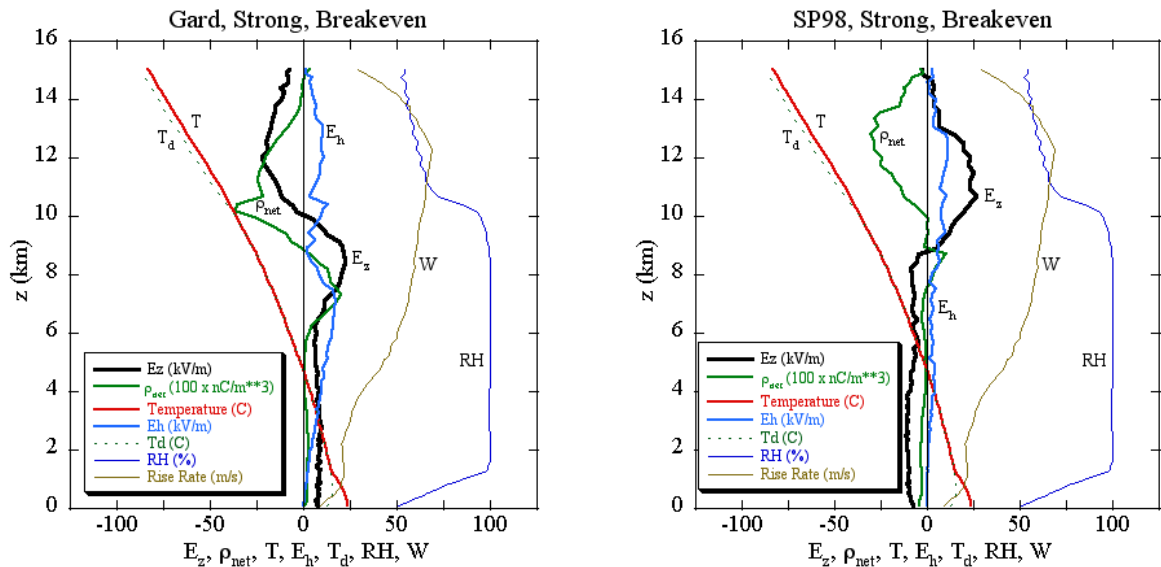


Fig. 4. Simulated electric field meter (EFM) sounding profiles through the main updraft of the Binger storm at 2h 23m for the (a - left) GARD and (b - right) SP98 non-inductive charging schemes. Launch time is 2h 23m, and the launch location is indicated by the heavy dot in Figure 2. The "rise rate" (W) is the sum of local updraft speed and the assumed 5 ms^{-1} parcel-relative upward speed of the Lagrangian point representing the "balloon".